Dielectric mirror optimization based on the phase-compensation method

O del Barco[1], I J Sola[2], E Conejero Jarque[2] and J M Bueno[1]

[1] Laboratorio de Óptica (LOUM), University of Murcia, E-30100 Murcia, Spain
[2] Grupo de Investigación en Aplicaciones del Láser y Fotónica (ALF-USAL), Departamento de Física Aplicada, University of Salamanca, E-37008 Salamanca, Spain

Abstract. A phase-compensation method is presented to fully optimize multilayer reflectance bandwidth, spectral phase and group delay dispersion (GDD). For a given multilayer (A), a set of different phase-compensated dielectric mirrors (B) is achieved as a function of a single parameter: the so-called reference wavelength λ_r. With a correct selection of the parameter λ_r, a set of different dielectric multilayers can be obtained with fixed broadband reflectance regions and smooth spectral phases (independently of the layers' thickness distribution) so that ultrashort pulses can be entirely reflected in such dielectric mirrors with a negligible amount of absorption and distortion. Hence, with an adequate numerical analysis via our phase-compensation method, experimental designs can be easily performed to obtain *ad hoc* dielectric mirrors for ultrashort pulse management.

1. Introduction

Multilayer periodic structures have been extensively used as high efficient mirrors over large selectable spectra. In this regard, photonic crystal devices based on thin film bilayers of TiO_2/SiO_2 [1] or Si/SiO_2 [2] have been designed to obtain omnidirectional reflection over the infrared spectrum. In the visible range, Deopura *et al.* [3] described a multilayer reflector formed by a stack of 19 alternating layers of tin (IV) sulfide and silica. Nevertheless, aperiodic multilayer structures not only can rival purely periodic multilayers in terms of basic properties such as very high selective transmission [4, 5], ultrabroad band reflection [6, 7, 8] or broadband filters [9], but also are widely used to manipulate light in different ways due to their structural flexibility. In particular, aperiodic multilayers have become a unique tool in ultrafast optics due to the way they can manage dispersion. Although early studies on dispersion properties of dielectric multilayer structures date back more than sixty years [10], it was the pioneering work by Szipöks and coworkers [11] which paved the way to the use of the so-called *chirped mirrors* in femtosecond lasers. In order to achieve few- or single-cycle ultrashort pulses, one must compensate the intrinsic dispersion introduced by linear propagation and the nonlinear processes responsible for the spectral broadening necessary to achieve such short pulses [12].

Dispersive multilayer mirrors (DMs) (for reviews on this subject see [13, 14, 15, 16] and references therein) are the preferred choice for that purpose due to several factors: First, it is possible to obtain a wide range of dispersion values together with high reflectivities and low absorption with relatively simple structures; moreover, both theoretical designs and optimization tools, and the fabrication techniques permit the design of their output in a very precise way; finally, as it happens in general with multilayer structures, they are scalable to different spectral regions provided that there are materials with adequate refractive indices. The use of DMs has permitted to obtain single-cycle and subcycle pulses with spectra spanning the visible and near infrared [17, 18, 19]. DMs in the extreme ultraviolet are also used to generate attosecond pulses [20, 21, 22]. In the opposite spectral region, due to recent advances in mid- and far-infrared laser sources, DMs have also gained interest in the last years [23, 24, 25]. Whereas high negative dispersion values may be desirable in order to compensate positive dispersion in the generation and compression of laser pulses, the opposite, i.e. low or near-zero dispersion, is the goal when we intend to use a mirror or a set of mirrors with an already compressed pulse [26, 27]. In addition to dielectric DMs, a family of different graphene-like heterostructures has achieved improved broadband nonlinear optical response for ultra-short pulse generation [28, 29]. Moreover, these promising materials might reduce the pulse transmission noise, boost the signal-to-noise ratio and reshape the deteriorated input signal [30].

In this article, we propose a technique to obtain phase-compensated dielectric multilayer mirrors which can operate in a wide spectral range in the mid-infrared. The plan of the work is as follows: in section 2 we develop the phase-compensation method based on the analytical calculation of the complex reflection amplitude $\widehat{r}_N$ of a general dielectric multilayer via the transfer matrix method (TMM). At a certain reference wavelength λ_r, a relation between

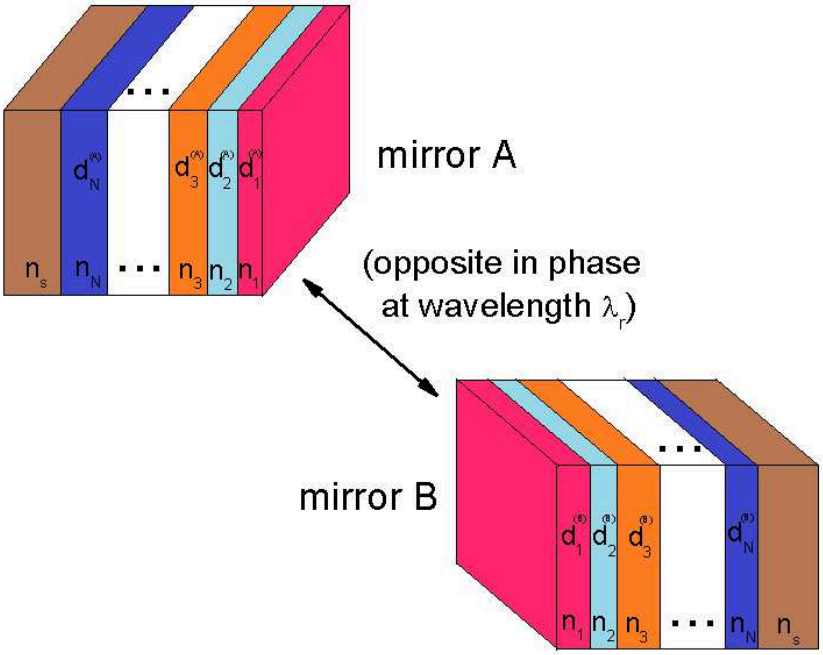

Figure 1. Schematic representation of two dielectric multilayers opposite in phase at the reference wavelength λ_r. Both mirrors are formed by N layers with refractive index n_k and the same substrate, but different layer thicknesses.

the thicknesses of two phase-compensated mirrors is found, providing a means to an entire enhancement of multilayer reflectance bandwidth and spectral phase. In section 3 we present some numerical results of dielectric mirror optimization (quarter-wavelength (QW), aperiodic and disordered multilayers) and ultrashort pulse propagation. Finally, we summarize our results and conclusions in section 4 and include an Appendix with details of the analytical calculation of $\widehat{r}_N$ (up to 5 layers) and mathematical induction for N layers.

2. Phase-compensation method

Let us consider a one-dimensional dielectric multilayer (A) formed by N layers of refractive index n_k and thickness $d_k^{(A)}$ on a substrate n_s (see Fig. 1). A multilayer (B) is similar to the previous one (that is, same refractive indices but different layer thicknesses $d_k^{(B)}$) but opposite in phase with (A) at wavelength λ_r. Our main goal is to derive an analytical expression for $d_k^{(B)}$, under this phase-compensation assumption, that will provide a systematic method to achieve broadband spectral regions where ultrashort pulses might be fully reflected without significant distortion.

For this purpose, let us now obtain an analytical expression for the complex reflection amplitude of a general dielectric multilayer $\widehat{r}_N$ via the transfer matrix method. A theoretical expression for $\widehat{r}_N$ is found by mathematical induction (see Appendix A for multilayers formed by 2, 3, 4 and 5 layers) which permits the spectral phase analysis required for phase-compensation. Defining the tilted optical admittance for the $k-th$ layer (η_k), the incident

medium (η_{in}) and substrate (η_s) as [38]

$$\eta_k = \begin{cases} \eta_0 n_k \cos\theta_k, & \text{s-polarization} \\ \eta_0 n_k / \cos\theta_k, & \text{p-polarization,} \end{cases} \tag{2.1}$$

$$\eta_{in,s} = \begin{cases} \eta_0 n_{in,s} \cos\theta_{in,s}, & \text{s-polarization} \\ \eta_0 n_{in,s} / \cos\theta_{in,s}, & \text{p-polarization,} \end{cases} \tag{2.2}$$

where η_0 is the admittance of free space and θ_k ($\theta_{in,s}$) corresponds to the refraction angle inside the layer (incident and exit angles), the analytical equation for the complex reflection amplitude $\widehat{r}_N$ can be written as

$$\widehat{r}_N = \frac{(\eta_{in} - \eta_s)\prod_{k=1}^{N} c_k + \sum_{j=1}^{N/2}(-1)^j a_j^{(-)} - i\sum_{j=1}^{(N+1)/2}(-1)^j b_j^{(-)}}{(\eta_{in} + \eta_s)\prod_{k=1}^{N} c_k + \sum_{j=1}^{N/2}(-1)^j a_j^{(+)} - i\sum_{j=1}^{(N+1)/2}(-1)^j b_j^{(+)}}. \tag{2.3}$$

For the sake of simplicity, we have defined the phase-term coefficients c_k and s_k in terms of the layer phase thicknesses δ_k

$$\begin{aligned} c_k &= \cos\delta_k = \cos\left(\frac{2\pi}{\lambda} n_k d_k \cos\theta_k\right) \\ s_k &= \sin\delta_k = \sin\left(\frac{2\pi}{\lambda} n_k d_k \cos\theta_k\right). \end{aligned} \tag{2.4}$$

The real part (RP) parameters $a_1^{(\pm)}$ in Eq. (2.3) are calculated as follows

$$a_1^{(\pm)} = \sum_{i=1}^{N}\sum_{k=i+1}^{N}\left[\left(\eta_{in}\frac{\eta_k}{\eta_i} \pm \eta_s\frac{\eta_i}{\eta_k}\right) s_i s_k \prod_{\substack{m=1 \\ m\neq i,k}}^{N-2} c_m\right], \tag{2.5}$$

where the number of summands in $a_1^{(\pm)}$ is a combination of N elements taken 2 at a time without repetition (that is, $C_{N,2} = \binom{N}{2}$). For $j = 2$, we have

$$a_2^{(\pm)} = \sum_{i=1}^{N}\sum_{k=i+1}^{N}\sum_{l=k+1}^{N}\sum_{n=l+1}^{N}\left[\left(\eta_{in}\frac{\eta_k\eta_n}{\eta_i\eta_l} \pm \eta_s\frac{\eta_i\eta_l}{\eta_k\eta_n}\right)\left(s_i s_k s_l s_n \prod_{\substack{m=1 \\ m\neq i,k,l,n}}^{N-4} c_m\right)\right] \tag{2.6}$$

and now there exist $C_{N,4}$ terms. For an even number of layers, an additional summand is obtained

$$a_{j=\frac{N}{2}}^{(\pm)} = \left(\frac{\eta_{in}\prod_{k=1}^{N/2}\eta_{2k}}{\prod_{k=0}^{(N-2)/2}\eta_{2k+1}} \pm \frac{\eta_s\prod_{k=0}^{(N-2)/2}\eta_{2k+1}}{\prod_{k=1}^{N/2}\eta_{2k}}\right)\prod_{m=1}^{N} s_m. \tag{2.7}$$

On the other hand, the imaginary part (IP) parameters can be computed by

$$b_1^{(\pm)} = \sum_{i=1}^{N} \left[\left(\frac{\eta_{in}\eta_s}{\eta_i} \pm \eta_i \right) \left(s_i \prod_{\substack{m=1 \\ m\neq i}}^{N-1} c_m \right) \right], \tag{2.8}$$

with $C_{N,1}$ terms and

$$b_2^{(\pm)} = \sum_{i=1}^{N} \sum_{k=i+1}^{N} \sum_{l=k+1}^{N} \left[\left(\frac{\eta_{in}\eta_s\eta_k}{\eta_i\eta_l} \pm \frac{\eta_i\eta_l}{\eta_k} \right) \left(s_i s_k s_l \prod_{\substack{m=1 \\ m\neq i,k,l}}^{N-3} c_m \right) \right], \tag{2.9}$$

where now we have $C_{N,3}$ summands. For an odd number of layers, there is one more term given by

$$b_{j=\frac{N+1}{2}}^{(\pm)} = \left(\frac{\eta_{in}\eta_s \prod_{k=1}^{(N-1)/2} \eta_{2k}}{\prod_{k=0}^{(N-1)/2} \eta_{2k+1}} \pm \frac{\prod_{k=0}^{(N-1)/2} \eta_{2k+1}}{\prod_{k=1}^{(N-1)/2} \eta_{2k}} \right) \prod_{m=1}^{N} s_m. \tag{2.10}$$

For higher orders ($j \geq 3$) the same combinatorial rule applies (as deduced in Appendix A for 4 and 5 layers and proven by mathematical induction). Hence, the total number of summands in both RP and IP (numerator and denominator of Eq. (2.3)) is $S_N = 2^{N-1}$.

As a direct consequence of its mathematical complexity, Eq. (2.3) is not a practical expression for an analytical calculation of $\widehat{r}_N$ but constitutes an useful tool for a theoretical analysis of the phase-compensation conditions. After inspection of this equation, one notices that it consists of a series of sines and cosines of δ_k depending on the layer optical admittances η_k. In order to achieve phase opposition, either the RP or the IP of both numerator and denominator of Eq. (2.3) must change their sign, but not simultaneously. Provided that the IP is a sum over an odd number of sine terms s_k and the RP over an even number of s_k, after some basic trigonometrical analysis we conclude that the phase thickness δ_k must shift to the nearest quadrant to an effective sign change. This phase-compensation condition can be expressed as

$$\delta_k^{(B)} = 2m\pi - \delta_k^{(A)}, \quad \text{for an integer } m \tag{2.11}$$

so, according to Eq. (2.4) and identifying the wavelength λ with λ_r we derive the following relation between phase-compensated mirror thicknesses

$$d_k^{(B)} = -d_k^{(A)} + \frac{m\lambda_r}{n_{k,r}}, \tag{2.12}$$

where $n_{k,r}$ is the refractive index of the $k-th$ layer at the reference wavelength λ_r. For simplicity, we selected normal incidence at both dielectric structures (i.e., $\theta_k = 0$). Despite this restrictive supposition, our numerical results won't change significatively as a function of the incident angle, as will be shown in section 3 for ultrashort pulse propagation.

It can be noticed that Eq. (2.12) relates the thicknesses of both phase-compensated multilayers and strongly depends on λ_r. For a fixed multilayer (A), a whole family of multilayers (B) can be created by varying just a single parameter: the reference wavelength λ_r (apart from the integer m). This useful tool allows an entire numerical study of the best phase-compensated multilayers compatible with broadband reflection bands and smooth values of the spectral phase.

3. Numerical results

In the previous section we presented the foundations of the phase-compensation method, being Eq. (2.12) the main result for a complete phase opposition between both mirrors. Let us now introduce some numerical results regarding multilayer parameters (reflectance and GDD) and ultrashort pulse propagation.

Accordingly, we show in Fig. 2 the spectral phase (left panels) and reflectance (right panels) of two QW phase-compensated mirrors (A) and (B) (42 layers) formed by the bilayer $\mathrm{Ge}/\mathrm{CaF_2}$ and Si as the substrate. The selected reference wavelength λ_r is 2921 nm and the angle of incidence varies from 0 to 45 degrees for s-polarization. As both multilayers are of quarter-wavelength type, the relation $n_H d_H = n_L d_L$ applies at λ_r, where H and L stand for the high and low refractive index layer (that is, Ge and $\mathrm{CaF_2}$, respectively). The thickness values for mirror (A) were chosen to be $d_H^{(A)} = 560.0$ nm and $d_L^{(A)} = 1597.2$ nm meanwhile for mirror (B), $d_H^{(B)} = 161.8$ nm and $d_L^{(B)} = 462.2$ nm (once calculated from Eq. (2.12) for the chosen reference wavelength and $m = 1$). It can be observed a significant improvement of reflectance and spectral phase for multilayer (B) even for different incident angles constituting a suitable mirror for ultrashort pulse management.

For a better visualization of multilayer optimization, we show in Fig. 3 two contour plots for mirror (B) (42 total number of layers formed by the bilayer $\mathrm{Ge}/\mathrm{CaF_2}$) where the GDD and reflectance (obtained numerically via the TMM) and represented versus the incident and reference wavelengths at normal incidence. As previously stated in Fig. 2, the widths of the different multilayers (B) have been calculated via Eq. (2.12). For each value of λ_r, a phase-compensated mirror (B) is generated creating a complete family of dielectric multilayers with selectable broadband spectral regions. The horizontal dashed line ($\lambda_r = 2921$ nm) corresponds to mirror (B) in Fig. 2 for $\theta = 0$ deg. It can be noticed that both reflectance and GDD present excellent properties in the region 2000 - 4000 nm.

The advantage of this phase-compensation method is that it is suitable for general dielectric multilayers (not only for periodic QW mirrors) and, therefore, aperiodic and disordered multilayer structures can be also optimized for ultrashort pulse processing. With this aim, a set of different phase-compensated mirrors (B) is presented in Fig. 4 where reflectance and GDD are shown versus the incident wavelength and λ_r for distinct aperiodic and disordered structures. Top panels correspond to linear increasing-width multilayers (IWM), a particular case of aperiodic structures where the layers' thicknesses increase linearly according to the following expressions [8]

$$d_{H,k}^{(B)} = d_{H,0}^{(B)} + a_H^{(B)} k, \qquad k = 3, 5, \ldots, N-1, \tag{3.1}$$

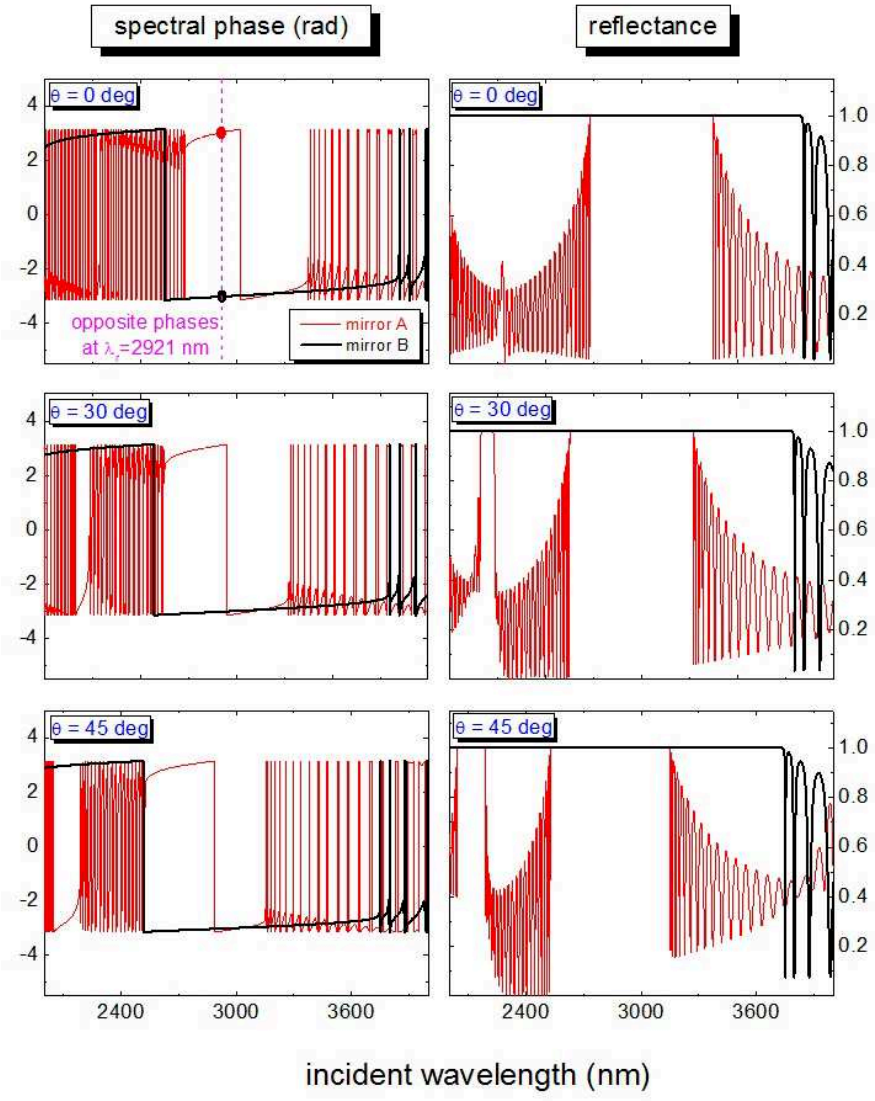

Figure 2. Spectral phase and reflectance of two QW phase-compensated mirrors (A) and (B) versus the incident wavelength. The total number of layers is 42 formed by the bilayer $\mathrm{Ge}/\mathrm{CaF}_2$ and Si as the substrate. At a reference wavelength $\lambda_r = 2921$ nm and normal incidence, both mirrors present opposite spectral phase.

$$d_{L,k}^{(B)} = d_{L,0}^{(B)} + a_L^{(B)} k, \qquad k = 4, 6, \ldots, N, \tag{3.2}$$

and the parameters $a_{H,L}^{(B)}$ stand for positive slopes of our IWM.

In agreement with Eq. (2.12), the phase-compensated mirrors (A) coincide with the so-called decreasing-width multilayers (DWM). In our particular case, the parameters of the original mirror (A) were chosen to be $d_{H,0}^{(A)} = 560.0$ nm, $d_{L,0}^{(A)} = 1597.2$ nm and $a_H^{(A)} = a_L^{(A)} = -5$ nm/layer, that is, a slow linear variation of the layers' thicknesses. One observes that, despite broadband reflectance regions are achieved upon an appropriate λ_r selection [8], the GDD does not match properly these spectral bands of high-reflectance. Hence, these aperiodic multilayer structures might not be adequate for ultrashort pulse propagation.

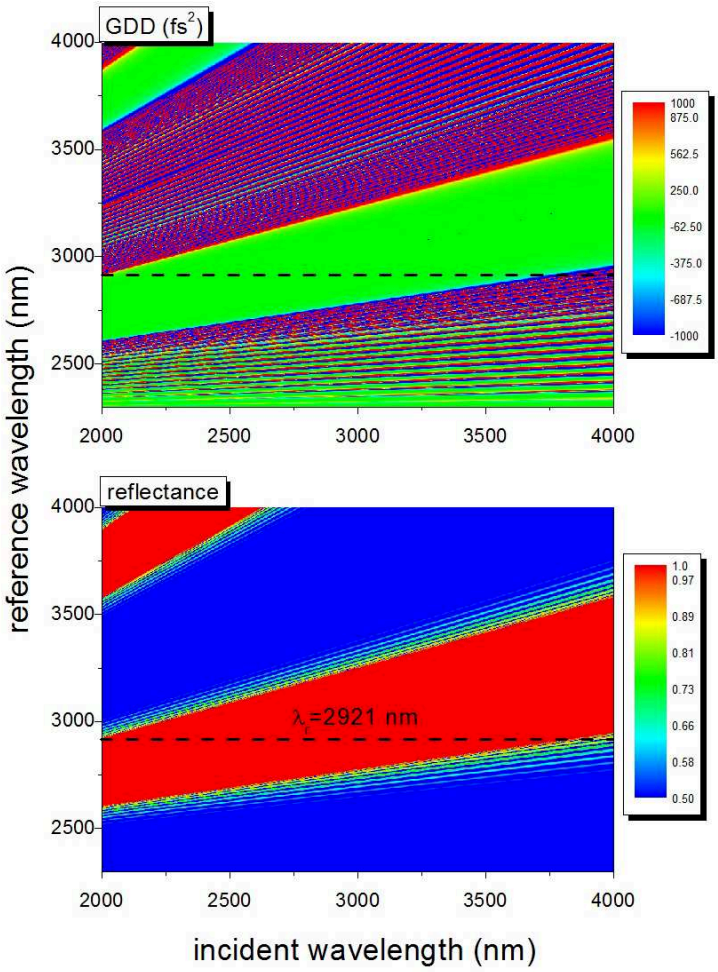

Figure 3. Group delay dispersion (GDD) and reflectance of $\mathrm{Ge/CaF_2}$ phase-compensated mirrors (B) versus the incident and reference wavelengths (normal incidence). For each value of λ_r a dielectric mirror (B) is obtained. The dashed line stands for mirror (B) depicted in Fig. 2.

On the other hand, disordered multilayers (with random variation of layers' thicknesses $d_k^{(B)}$ around a central value) can also be studied with our phase-compensation method. Under these conditions, we have

$$d_k^{(B)} = d_{k,0}^{(B)} + \xi_k \delta, \qquad k = 1, \ldots, N, \tag{3.3}$$

where ξ_k are zero-mean independent random numbers within the interval $[-0.5, 0.5]$ and the parameter δ measures the strength of the disorder. In this sense, Fig. 4 exhibits two cases of disordered mirrors (B) (42 total number of alternating $\mathrm{Ge/CaF_2}$ layers) where the percentage of random thickness variation was up to 40% (strong disorder, central panels) and 10% (weak disorder, bottom panels) for a phase-compensated mirror (A) with mean thickness values $d_H^{(A)} = 560.0$ nm and $d_L^{(A)} = 1597.2$ nm. A similar situation to the aperiodic IWMs occurs to the strong-disordered case, where both reflectance and GDD spectral regions mismatch (compare bottom panels in Fig. 4). Nevertheless, for our weak-disordered case a

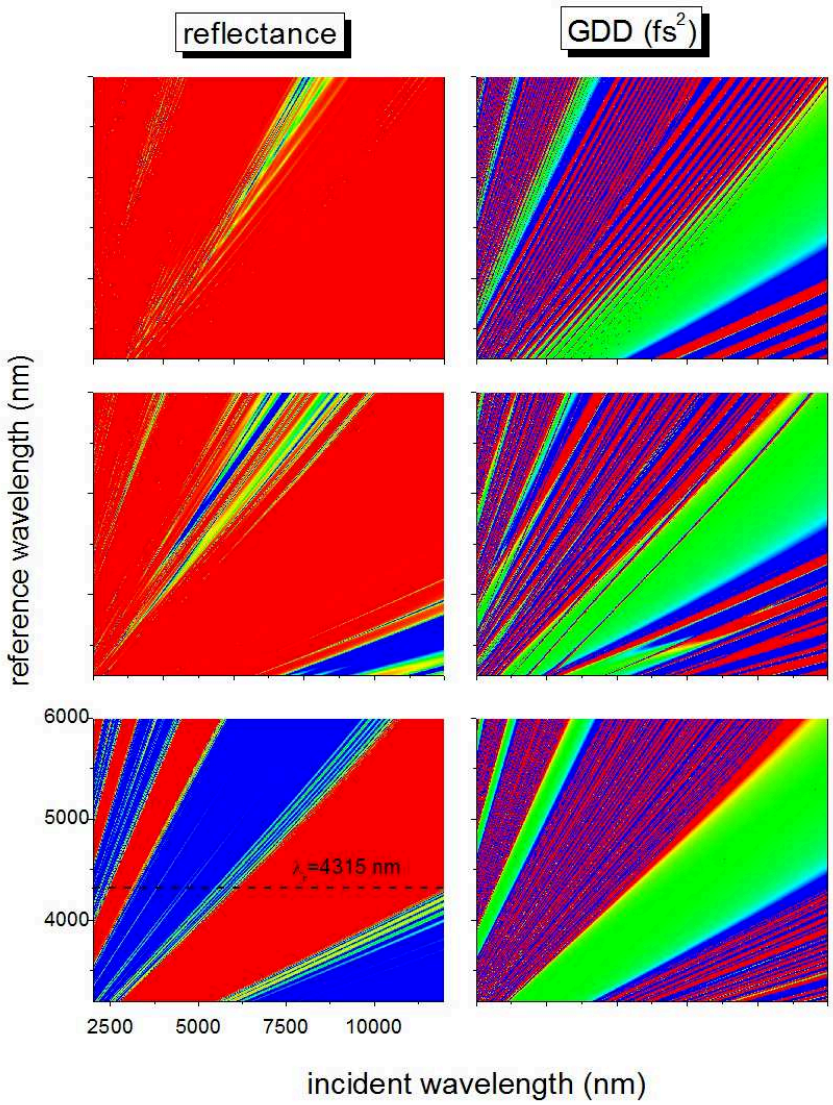

Figure 4. Reflectance (left panels) and GDD (right panels) versus the incident and reference wavelengths for different aperiodic and disordered $\mathrm{Ge}/\mathrm{CaF}_2$ phase-compensated multilayers (B) (colorbar the same as in Fig. 3). Top panels represent aperiodic IWMs while central and bottom panels correspond to strong and weak disordered multilayers (see text), respectively. The dashed line at $\lambda_r = 4315$ nm in the weak-disordered case shows the spectral bandwidth for ultrashort pulse reflection (as discussed in next figure).

remarkable concordance between both magnitudes is achieved, being probably the best (and more realistic) candidate for ultrashort pulse management.

Finally, let us now analyze the response of an ultrashort gaussian pulse when it is reflected on an optimized dielectric mirror (B). For an incident gaussian pulse $A(\omega)$ centered at the frequency ω_0 and Full Width at Half Maximum (FWHM) $\Delta\omega$

$$A(\omega) = \frac{A_0\, 0.375\sqrt{\pi}}{\Delta\omega} \exp\left[-\frac{0.375\pi}{\Delta\omega}(\omega-\omega_0)\right]^2, \tag{3.4}$$

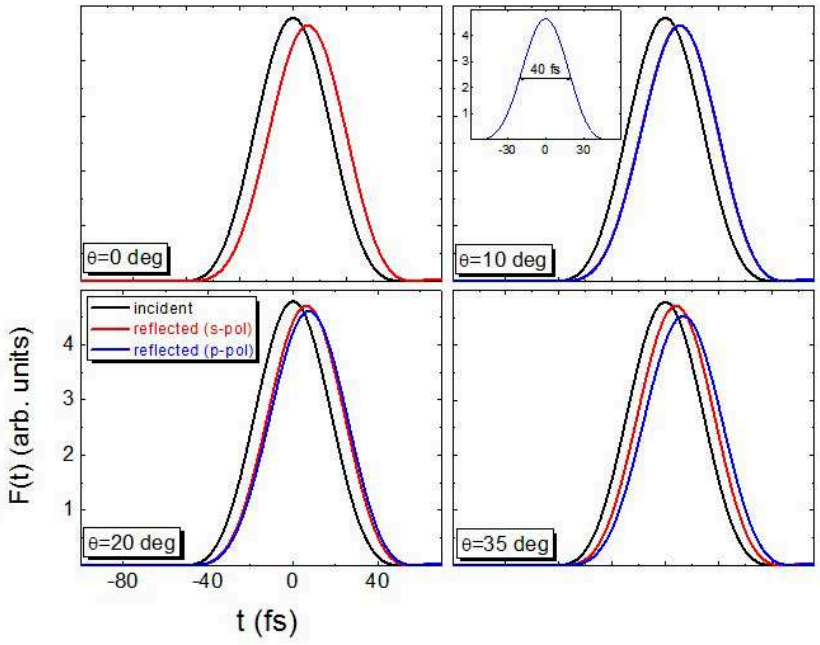

Figure 5. An ultrashort gaussian pulse $F(t)$ (amplitude in arbitrary units) reflected on a phase-compensated mirror (B) (determined by $\lambda_r = 4315$ nm in Fig. 4) for different incident angles. The central wavelength and pulse FWHM were selected as 8017 nm and 40 fs, respectively, so it corresponds to a 1.5-cycle ultrashort pulse.

the Fourier transform of Eq. (3.4) provides us the general expression for the time-dependent gaussian pulse $F(t)$ [31]

$$F(t) = \int_{-\infty}^{\infty} \mathrm{d}\omega\, \widehat{r}_N(\omega) A(\omega) \exp[i\omega t], \tag{3.5}$$

where $\widehat{r}_N(\omega)$ represents the complex reflection amplitude of mirror (B) (calculated numerically via the TMM).

In Fig. 5 we consider a 1.5-cycle gaussian pulse (centered at 8017 nm and temporal FWHM 40 fs) reflected on a weak-disordered mirror (B) determined by the reference wavelength $\lambda_r = 4315$ nm depicted in Fig. 4 (bottom panels). The reflected pulse envelope is represented for both s and p-polarizations and different incident angles. The pulse shapes do not suffer distortion after reflection on multilayer (B) except in the case of the p-polarized pulse at 35 degrees incidence angle, which is slightly distorted. Subsequently, an appropriate amount of disorder in dielectric multilayers might be also beneficial for ultrashort pulse managing.

It is important to remark that the results obtained in this work are helpful in a wide spectral range by choosing adequate materials. However, in the case of high power lasers one needs to take into account the possible nonlinear response of the materials, mainly Kerr effect [32] and two-photon absorption [33] and include it in the design process to obtain more accurate dispersion results. Regarding Kerr effect, it induces a change in the refractive index of the layers which slightly affects their optical thicknesses. Since the optical response of our

structure is not affected by small changes in the layer thicknesses, Kerr effect is not expected to be a limiting factor. On the other hand, if the fluence is in the range of a few $\mathrm{J/cm^2}$, as it happens with multilayer dielectric mirrors used in multi-terawatt and petawatt laser systems, a study of the laser induced damage threshold of the mirror is also necessary [34, 35, 36, 37].

4. Conclusions

A simple phase-compensation method has been developed to optimize multilayer bandwidth, spectral phase and group delay dispersion at a given spectral region. Thus, mirrors can be designed *ad hoc* following the procedure to manage ultrashort pulses. For a given dielectric mirror (A), a set of multilayers (B) with the same refractive indices as (A) but opposite in phase is achieved at a certain reference wavelength λ_r (see again Eq. (2.12)). With the correct selection of the parameter λ_r, one can select phase-compensated mirrors (B) where both reflectance and GDD present the same adequate broadband spectral regions for ultrashort pulse propagation.

As shown in Fig. 5, we achieved 40-fs gaussian pulses almost totally reflected on weak-disordered mirrors (angles of incidence up to 35 degrees) without significant distortion. It is worth mentioning that, although multilayers (B) are generated to compensate the spectral phase of mirrors (A) at a given λ_r, both dielectric structures do not act together as a pair of phase-compensated mirrors with null GDD. In other words, the combination of a multilayer pair (A) + (B) is less efficient than a single mirror (B) alone. Despite QW periodic mirrors have been widely manufactured as efficient ultrashort pulse reflectors, we have demonstrated that a proper amount of disorder in these mirrors does not affect their reflectance and phase properties. Therefore, weak-disordered mirrors might be designed as totally qualified ultrashort pulse reflectors providing a means to reduce costs in multilayer production. This kind of mirrors can be very hepfull to manage the propagation of ultrashort pulses specially in the mid-IR spectral region, a very active topic nowadays.

It should be noted that, despite the theoretical nature of the main results described in the article, a complete implementation into an experimental design can be performed. Firstly, a pair of proper dielectric materials and a generic multilayer (A) must be selected. Then, the thicknesses of the optimized multilayers (B) should be calculated via Eq. (2.12) and a complete representation of the reflectance and GDD is obtained numerically as a function of the parameter λ_r (similar to Fig. 3). Finally, the researcher must select the appropriate value of λ_r according to the desired wavelength range. In other words, with an adequate numerical analysis via our phase-compensation method, experimental designs can be easily performed to obtain *ad hoc* dielectric mirrors for ultrashort pulse management.

Acknowledgments

O. del Barco acknowledges Almudena Nicolás for interesting discussions on ultrashort pulse processing in QW periodic multilayers. The authors appreciate the contribution of Dr. Thomas Mayer to the revision of the manuscript and thank support from Spanish Ministerio

de Economía y Competitividad (Grants FIS2015-71933-REDT, FIS2016-75652-P, FIS2017-87970-R, FIS2016-76163-R), Spanish Ministerio de Ciencia, Innovación y Universidades (Grant EQC2018-004117-P) and from Junta de Castilla y León (Grant SA287P18).

Appendix A. Analytical calculation of $\widehat{r}_N$ (up to 5 layers)

Let us first consider a single dielectric layer of thickness d_1 and refractive index n_1. The characteristic matrix of this thin film is given by [38]

$$\begin{pmatrix} \cos\delta_1 & (i\sin\delta_1)/\eta_1 \\ i\eta_1\sin\delta_1 & \cos\delta_1 \end{pmatrix}, \tag{A.1}$$

where $\delta_1 = (2\pi/\lambda)n_1 d_1\cos\theta_1$ corresponds to the phase thickness (θ_1 is the refraction angle inside the layer), η_0 the admittance of free space and η_1 the tilted optical admittance of the thin film

$$\eta_1 = \begin{cases} \eta_0 n_1\cos\theta_1, & \text{s-polarization} \\ \eta_0 n_1/\cos\theta_1, & \text{p-polarization.} \end{cases} \tag{A.2}$$

Equivalently, for the incident medium and substrate, we have

$$\eta_{in,s} = \begin{cases} \eta_0 n_{in,s}\cos\theta_{in,s}, & \text{s-polarization} \\ \eta_0 n_{in,s}/\cos\theta_{in,s}, & \text{p-polarization,} \end{cases} \tag{A.3}$$

where $\theta_{in,s}$ corresponds to the incident and exit angles on the single layer, respectively.

In order to derive an analytical expression for the complex reflection amplitude $\widehat{r}_1$, we set the following matrix equation

$$\begin{pmatrix} B \\ C \end{pmatrix} = \begin{pmatrix} \cos\delta_1 & (i\sin\delta_1)/\eta_1 \\ i\eta_1\sin\delta_1 & \cos\delta_1 \end{pmatrix} \begin{pmatrix} 1 \\ \eta_s \end{pmatrix}, \tag{A.4}$$

and the complex reflection amplitude for a single layer $\widehat{r}_1$ is given by [38]

$$\widehat{r}_1 = \frac{B\eta_{in} - C}{B\eta_{in} + C}. \tag{A.5}$$

After some basic algebra, Eq. (A.5) is written as

$$\widehat{r}_1 = \frac{\eta_1\left(\eta_{in} - \eta_s\right)c_1 + i\left(\eta_{in}\eta_s - \eta_1^2\right)s_1}{\eta_1\left(\eta_{in} + \eta_s\right)c_1 + i\left(\eta_{in}\eta_s + \eta_1^2\right)s_1}, \tag{A.6}$$

where $c_1 = \cos\delta_1$ and $s_1 = \sin\delta_1$.

Let another layer be added to the previous single film (with parameters n_2 and d_2). The final matrix equation is similar to Eq. (A.4) but now the characteristic matrix is calculated by the product of the two corresponding matrices

$$\begin{pmatrix} B \\ C \end{pmatrix} = \prod_{k=1}^{2} \begin{pmatrix} \cos\delta_k & (i\sin\delta_k)/\eta_k \\ i\eta_k\sin\delta_k & \cos\delta_k \end{pmatrix} \begin{pmatrix} 1 \\ \eta_s \end{pmatrix}. \tag{A.7}$$

In this case, the complex reflection amplitude $\widehat{r}_2$ turns out to be

$$\widehat{r}_2 = \frac{\widehat{A}_2}{\widehat{B}_2}, \tag{A.8}$$

where

$$\widehat{A}_2 = (\eta_{in} - \eta_s)\, c_1 c_2 + \left(\frac{\eta_s \eta_1}{\eta_2} - \frac{\eta_{in}\eta_2}{\eta_1}\right) s_1 s_2 + i \left[\left(\frac{\eta_{in}\eta_s}{\eta_1} - \eta_1\right) s_1 c_2 + \left(\frac{\eta_{in}\eta_s}{\eta_2} - \eta_2\right) c_1 s_2\right], \tag{A.9}$$

and

$$\widehat{B}_2 = (\eta_{in} + \eta_s)\, c_1 c_2 - \left(\frac{\eta_s \eta_1}{\eta_2} + \frac{\eta_{in}\eta_2}{\eta_1}\right) s_1 s_2 + i \left[\left(\frac{\eta_{in}\eta_s}{\eta_1} + \eta_1\right) s_1 c_2 + \left(\frac{\eta_{in}\eta_s}{\eta_2} + \eta_2\right) c_1 s_2\right]. \tag{A.10}$$

Appendix A.1. Three and four layers

By an iterative process, the following expressions for three and four layers (with respective parameters n_3, d_3 and n_4, d_4) are derived

$$\widehat{r}_3 = \frac{\widehat{A}_3}{\widehat{B}_3}, \tag{A.11}$$

where the numerator

$$\widehat{A}_3 = (\eta_{in} - \eta_s)\, c_1 c_2 c_3 + \left(\frac{\eta_s \eta_1}{\eta_2} - \frac{\eta_{in}\eta_2}{\eta_1}\right) s_1 s_2 c_3 + \left(\frac{\eta_s \eta_1}{\eta_3} - \frac{\eta_{in}\eta_3}{\eta_1}\right) s_1 c_2 s_3 + \left(\frac{\eta_s \eta_2}{\eta_3} - \frac{\eta_{in}\eta_3}{\eta_2}\right) c_1 s_2 s_3 + i \left[\left(\frac{\eta_{in}\eta_s}{\eta_1} - \eta_1\right) s_1 c_2 c_3 + \left(\frac{\eta_{in}\eta_s}{\eta_2} - \eta_2\right) c_1 s_2 c_3 + \left(\frac{\eta_{in}\eta_s}{\eta_3} - \eta_3\right) c_1 c_2 s_3 + \left(\frac{\eta_3 \eta_1}{\eta_2} - \frac{\eta_{in}\eta_s\eta_2}{\eta_1\eta_3}\right) s_1 s_2 s_3\right], \tag{A.12}$$

and the denominator

$$\widehat{B}_3 = (\eta_{in} + \eta_s)\, c_1 c_2 c_3 - \left(\frac{\eta_s \eta_1}{\eta_2} + \frac{\eta_{in}\eta_2}{\eta_1}\right) s_1 s_2 c_3 - \left(\frac{\eta_s \eta_1}{\eta_3} + \frac{\eta_{in}\eta_3}{\eta_1}\right) s_1 c_2 s_3 - \left(\frac{\eta_s \eta_2}{\eta_3} + \frac{\eta_{in}\eta_3}{\eta_2}\right) c_1 s_2 s_3 + i \left[\left(\frac{\eta_{in}\eta_s}{\eta_1} + \eta_1\right) s_1 c_2 c_3 + \left(\frac{\eta_{in}\eta_s}{\eta_2} + \eta_2\right) c_1 s_2 c_3 + \left(\frac{\eta_{in}\eta_s}{\eta_3} + \eta_3\right) c_1 c_2 s_3 - \left(\frac{\eta_3 \eta_1}{\eta_2} + \frac{\eta_{in}\eta_s\eta_2}{\eta_1\eta_3}\right) s_1 s_2 s_3\right]. \tag{A.13}$$

Both numerator and denominator contain $1 + \binom{3}{2} = 4$ summands (for the RP) and $\binom{3}{1} + \binom{3}{3} = 4$ terms for the IP (where, for simplicity, the binomial expressions are expressed as combinations of N elements taken j at a time without repetition, i.e., $C_{N,j} = \binom{N}{j}$). Namely, the number of terms for both real and imaginary parts is $S_3 = 2^2$.

For a multilayer formed by four layers

$$\widehat{r}_4 = \frac{\widehat{A}_4}{\widehat{B}_4}, \tag{A.14}$$

where

$$\begin{aligned}
\widehat{A}_4 &= (\eta_{in} - \eta_s)\, c_1c_2c_3c_4 + \left(\frac{\eta_s\eta_1}{\eta_2} - \frac{\eta_{in}\eta_2}{\eta_1}\right) s_1s_2c_3c_4 + \left(\frac{\eta_s\eta_1}{\eta_3} - \frac{\eta_{in}\eta_3}{\eta_1}\right) s_1c_2s_3c_4 \\
&+ \left(\frac{\eta_s\eta_1}{\eta_4} - \frac{\eta_{in}\eta_4}{\eta_1}\right) s_1c_2c_3s_4 + \left(\frac{\eta_s\eta_2}{\eta_3} - \frac{\eta_{in}\eta_3}{\eta_2}\right) c_1s_2s_3c_4 + \left(\frac{\eta_s\eta_2}{\eta_4} - \frac{\eta_{in}\eta_4}{\eta_2}\right) c_1s_2c_3s_4 \\
&+ \left(\frac{\eta_s\eta_3}{\eta_4} - \frac{\eta_{in}\eta_4}{\eta_3}\right) c_1c_2s_3s_4 + \left(\frac{\eta_{in}\eta_2\eta_4}{\eta_1\eta_3} - \frac{\eta_s\eta_1\eta_3}{\eta_2\eta_4}\right) s_1s_2s_3s_4 \\
&+ i\left[\left(\frac{\eta_{in}\eta_s}{\eta_1} - \eta_1\right) s_1c_2c_3c_4 + \left(\frac{\eta_{in}\eta_s}{\eta_2} - \eta_2\right) c_1s_2c_3c_4 + \left(\frac{\eta_{in}\eta_s}{\eta_3} - \eta_3\right) c_1c_2s_3c_4\right. \\
&+ \left(\frac{\eta_{in}\eta_s}{\eta_4} - \eta_4\right) c_1c_2c_3s_4 + \left(\frac{-\eta_{in}\eta_s\eta_2}{\eta_1\eta_3} + \frac{\eta_1\eta_3}{\eta_2}\right) s_1s_2s_3c_4 + \left(\frac{-\eta_{in}\eta_s\eta_2}{\eta_1\eta_4} + \frac{\eta_1\eta_4}{\eta_2}\right) s_1s_2c_3s_4 \\
&+ \left.\left(\frac{-\eta_{in}\eta_s\eta_3}{\eta_1\eta_4} + \frac{\eta_1\eta_4}{\eta_3}\right) s_1c_2s_3s_4 + \left(\frac{-\eta_{in}\eta_s\eta_3}{\eta_2\eta_4} + \frac{\eta_2\eta_4}{\eta_3}\right) c_1s_2s_3s_4\right],
\end{aligned} \tag{A.15}$$

and

$$\begin{aligned}
\widehat{B}_4 &= (\eta_{in} + \eta_s)\, c_1c_2c_3c_4 - \left(\frac{\eta_s\eta_1}{\eta_2} + \frac{\eta_{in}\eta_2}{\eta_1}\right) s_1s_2c_3c_4 - \left(\frac{\eta_s\eta_1}{\eta_3} + \frac{\eta_{in}\eta_3}{\eta_1}\right) s_1c_2s_3c_4 \\
&- \left(\frac{\eta_s\eta_1}{\eta_4} + \frac{\eta_{in}\eta_4}{\eta_1}\right) s_1c_2c_3s_4 - \left(\frac{\eta_s\eta_2}{\eta_3} + \frac{\eta_{in}\eta_3}{\eta_2}\right) c_1s_2s_3c_4 - \left(\frac{\eta_s\eta_2}{\eta_4} + \frac{\eta_{in}\eta_4}{\eta_2}\right) c_1s_2c_3s_4 \\
&- \left(\frac{\eta_s\eta_3}{\eta_4} + \frac{\eta_{in}\eta_4}{\eta_3}\right) c_1c_2s_3s_4 + \left(\frac{\eta_{in}\eta_2\eta_4}{\eta_1\eta_3} + \frac{\eta_s\eta_1\eta_3}{\eta_2\eta_4}\right) s_1s_2s_3s_4 \\
&+ i\left[\left(\frac{\eta_{in}\eta_s}{\eta_1} + \eta_1\right) s_1c_2c_3c_4 + \left(\frac{\eta_{in}\eta_s}{\eta_2} + \eta_2\right) c_1s_2c_3c_4 + \left(\frac{\eta_{in}\eta_s}{\eta_3} + \eta_3\right) c_1c_2s_3c_4\right. \\
&+ \left(\frac{\eta_{in}\eta_s}{\eta_4} + \eta_4\right) c_1c_2c_3s_4 - \left(\frac{\eta_{in}\eta_s\eta_2}{\eta_1\eta_3} + \frac{\eta_1\eta_3}{\eta_2}\right) s_1s_2s_3c_4 - \left(\frac{\eta_{in}\eta_s\eta_2}{\eta_1\eta_4} + \frac{\eta_1\eta_4}{\eta_2}\right) s_1s_2c_3s_4 \\
&- \left.\left(\frac{\eta_{in}\eta_s\eta_3}{\eta_1\eta_4} + \frac{\eta_1\eta_4}{\eta_3}\right) s_1c_2s_3s_4 \left(\frac{\eta_{in}\eta_s\eta_3}{\eta_2\eta_4} + \frac{\eta_2\eta_4}{\eta_3}\right) c_1s_2s_3s_4\right].
\end{aligned} \tag{A.16}$$

In this case, the number of summands in both numerator and denominator results to be $1 + C_{4,2} + C_{4,4} = 8$ (for the RP) and $C_{4,1} + C_{4,3} = 8$ for the IP (that is, $S_4 = 2^3$ terms).

Appendix A.2. Five layers

After more tedious calculations, the analytical expression for $\widehat{r}_5$ was found to be

$$\widehat{r}_5 = \frac{\widehat{A}_5}{\widehat{B}_5}, \tag{A.17}$$

where

$$\widehat{A}_5 = (\eta_{in} - \eta_s)\, c_1c_2c_3c_4c_5 + \left(\frac{\eta_s\eta_1}{\eta_2} - \frac{\eta_{in}\eta_2}{\eta_1}\right) s_1s_2c_3c_4c_5 + \left(\frac{\eta_s\eta_1}{\eta_3} - \frac{\eta_{in}\eta_3}{\eta_1}\right) s_1c_2s_3c_4c_5$$
$$+ \left(\frac{\eta_s\eta_1}{\eta_4} - \frac{\eta_{in}\eta_4}{\eta_1}\right) s_1c_2c_3s_4c_5 + \left(\frac{\eta_s\eta_1}{\eta_5} - \frac{\eta_{in}\eta_5}{\eta_1}\right) s_1c_2c_3c_4s_5 + \left(\frac{\eta_s\eta_2}{\eta_3} - \frac{\eta_{in}\eta_3}{\eta_2}\right) c_1s_2s_3c_4c_5$$
$$+ \left(\frac{\eta_s\eta_2}{\eta_4} - \frac{\eta_{in}\eta_4}{\eta_2}\right) c_1s_2c_3s_4c_5 + \left(\frac{\eta_s\eta_2}{\eta_5} - \frac{\eta_{in}\eta_5}{\eta_2}\right) c_1s_2c_3c_4s_5 + \left(\frac{\eta_s\eta_3}{\eta_4} - \frac{\eta_{in}\eta_4}{\eta_3}\right) c_1c_2s_3s_4c_5$$
$$+ \left(\frac{\eta_s\eta_3}{\eta_5} - \frac{\eta_{in}\eta_5}{\eta_3}\right) c_1c_2s_3c_4s_5 + \left(\frac{\eta_s\eta_4}{\eta_5} - \frac{\eta_{in}\eta_5}{\eta_4}\right) c_1c_2c_3s_4s_5$$
$$+ \left(\frac{\eta_{in}\eta_2\eta_4}{\eta_1\eta_3} - \frac{\eta_s\eta_1\eta_3}{\eta_2\eta_4}\right) s_1s_2s_3s_4c_5 + \left(\frac{\eta_{in}\eta_2\eta_5}{\eta_1\eta_3} - \frac{\eta_s\eta_1\eta_3}{\eta_2\eta_5}\right) s_1s_2s_3c_4s_5$$
$$+ \left(\frac{\eta_{in}\eta_2\eta_5}{\eta_1\eta_4} - \frac{\eta_s\eta_1\eta_4}{\eta_2\eta_5}\right) s_1s_2c_3s_4s_5 + \left(\frac{\eta_{in}\eta_3\eta_5}{\eta_1\eta_4} - \frac{\eta_s\eta_1\eta_4}{\eta_3\eta_5}\right) s_1c_2s_3s_4s_5$$
$$+ \left(\frac{\eta_{in}\eta_3\eta_5}{\eta_2\eta_4} - \frac{\eta_s\eta_2\eta_4}{\eta_3\eta_5}\right) c_1s_2s_3s_4s_5 + i\left[\left(\frac{\eta_{in}\eta_s}{\eta_1} - \eta_1\right) s_1c_2c_3c_4c_5\right.$$
$$+ \left(\frac{\eta_{in}\eta_s}{\eta_2} - \eta_2\right) c_1s_2c_3c_4c_5 + \left(\frac{\eta_{in}\eta_s}{\eta_3} - \eta_3\right) c_1c_2s_3c_4c_5$$
$$+ \left(\frac{\eta_{in}\eta_s}{\eta_4} - \eta_4\right) c_1c_2c_3s_4c_5 + \left(\frac{\eta_{in}\eta_s}{\eta_5} - \eta_5\right) c_1c_2c_3c_4s_5$$
$$+ \left(\frac{-\eta_{in}\eta_s\eta_2}{\eta_1\eta_3} + \frac{\eta_1\eta_3}{\eta_2}\right) s_1s_2s_3c_4c_5 + \left(\frac{-\eta_{in}\eta_s\eta_2}{\eta_1\eta_4} + \frac{\eta_1\eta_4}{\eta_2}\right) s_1s_2c_3s_4c_5$$
$$+ \left(\frac{-\eta_{in}\eta_s\eta_2}{\eta_1\eta_5} + \frac{\eta_1\eta_5}{\eta_2}\right) s_1s_2c_3c_4s_5 + \left(\frac{-\eta_{in}\eta_s\eta_3}{\eta_1\eta_4} + \frac{\eta_1\eta_4}{\eta_3}\right) s_1c_2s_3s_4c_5$$
$$+ \left(\frac{-\eta_{in}\eta_s\eta_3}{\eta_1\eta_5} + \frac{\eta_1\eta_5}{\eta_3}\right) s_1c_2s_3c_4s_5 + \left(\frac{-\eta_{in}\eta_s\eta_4}{\eta_1\eta_5} + \frac{\eta_1\eta_5}{\eta_4}\right) s_1c_2c_3s_4s_5$$
$$+ \left(\frac{-\eta_{in}\eta_s\eta_3}{\eta_2\eta_4} + \frac{\eta_2\eta_4}{\eta_3}\right) c_1s_2s_3s_4c_5 + \left(\frac{-\eta_{in}\eta_s\eta_3}{\eta_2\eta_5} + \frac{\eta_2\eta_5}{\eta_3}\right) c_1s_2s_3c_4s_5$$
$$+ \left(\frac{-\eta_{in}\eta_s\eta_4}{\eta_2\eta_5} + \frac{\eta_2\eta_5}{\eta_4}\right) c_1s_2c_3s_4s_5 + \left(\frac{-\eta_{in}\eta_s\eta_4}{\eta_3\eta_5} + \frac{\eta_3\eta_5}{\eta_4}\right) c_1c_2s_3s_4s_5$$
$$\left. + \left(\frac{\eta_{in}\eta_s\eta_2\eta_4}{\eta_1\eta_3\eta_5} - \frac{\eta_1\eta_3\eta_5}{\eta_2\eta_4}\right) s_1s_2s_3s_4s_5\right], \tag{A.18}$$

and

$$\widehat{B}_5 = (\eta_{in}+\eta_s)\,c_1c_2c_3c_4c_5 - \left(\frac{\eta_s\eta_1}{\eta_2}+\frac{\eta_{in}\eta_2}{\eta_1}\right)s_1s_2c_3c_4c_5 - \left(\frac{\eta_s\eta_1}{\eta_3}+\frac{\eta_{in}\eta_3}{\eta_1}\right)s_1c_2s_3c_4c_5$$
$$- \left(\frac{\eta_s\eta_1}{\eta_4}+\frac{\eta_{in}\eta_4}{\eta_1}\right)s_1c_2c_3s_4c_5 - \left(\frac{\eta_s\eta_1}{\eta_5}+\frac{\eta_{in}\eta_5}{\eta_1}\right)s_1c_2c_3c_4s_5 - \left(\frac{\eta_s\eta_2}{\eta_3}+\frac{\eta_{in}\eta_3}{\eta_2}\right)c_1s_2s_3c_4c_5$$
$$- \left(\frac{\eta_s\eta_2}{\eta_4}+\frac{\eta_{in}\eta_4}{\eta_2}\right)c_1s_2c_3s_4c_5 - \left(\frac{\eta_s\eta_2}{\eta_5}+\frac{\eta_{in}\eta_5}{\eta_2}\right)c_1s_2c_3c_4s_5 - \left(\frac{\eta_s\eta_3}{\eta_4}+\frac{\eta_{in}\eta_4}{\eta_3}\right)c_1c_2s_3s_4c_5$$
$$- \left(\frac{\eta_s\eta_3}{\eta_5}+\frac{\eta_{in}\eta_5}{\eta_3}\right)c_1c_2s_3c_4s_5 - \left(\frac{\eta_s\eta_4}{\eta_5}+\frac{\eta_{in}\eta_5}{\eta_4}\right)c_1c_2c_3s_4s_5$$
$$+ \left(\frac{\eta_{in}\eta_2\eta_4}{\eta_1\eta_3}+\frac{\eta_s\eta_1\eta_3}{\eta_2\eta_4}\right)s_1s_2s_3s_4c_5 + \left(\frac{\eta_{in}\eta_2\eta_5}{\eta_1\eta_3}+\frac{\eta_s\eta_1\eta_3}{\eta_2\eta_5}\right)s_1s_2s_3c_4s_5$$
$$+ \left(\frac{\eta_{in}\eta_2\eta_5}{\eta_1\eta_4}+\frac{\eta_s\eta_1\eta_4}{\eta_2\eta_5}\right)s_1s_2c_3s_4s_5 + \left(\frac{\eta_{in}\eta_3\eta_5}{\eta_1\eta_4}+\frac{\eta_s\eta_1\eta_4}{\eta_3\eta_5}\right)s_1c_2s_3s_4s_5$$
$$+ \left(\frac{\eta_{in}\eta_3\eta_5}{\eta_2\eta_4}+\frac{\eta_s\eta_2\eta_4}{\eta_3\eta_5}\right)c_1s_2s_3s_4s_5 + i\left[\left(\frac{\eta_{in}\eta_s}{\eta_1}+\eta_1\right)s_1c_2c_3c_4c_5\right.$$
$$+ \left(\frac{\eta_{in}\eta_s}{\eta_2}+\eta_2\right)c_1s_2c_3c_4c_5 + \left(\frac{\eta_{in}\eta_s}{\eta_3}+\eta_3\right)c_1c_2s_3c_4c_5$$
$$+ \left(\frac{\eta_{in}\eta_s}{\eta_4}+\eta_4\right)c_1c_2c_3s_4c_5 + \left(\frac{\eta_{in}\eta_s}{\eta_5}+\eta_5\right)c_1c_2c_3c_4s_5$$
$$- \left(\frac{\eta_{in}\eta_s\eta_2}{\eta_1\eta_3}+\frac{\eta_1\eta_3}{\eta_2}\right)s_1s_2s_3c_4c_5 - \left(\frac{\eta_{in}\eta_s\eta_2}{\eta_1\eta_4}+\frac{\eta_1\eta_4}{\eta_2}\right)s_1s_2c_3s_4c_5$$
$$- \left(\frac{\eta_{in}\eta_s\eta_2}{\eta_1\eta_5}+\frac{\eta_1\eta_5}{\eta_2}\right)s_1s_2c_3c_4s_5 - \left(\frac{\eta_{in}\eta_s\eta_3}{\eta_1\eta_4}+\frac{\eta_1\eta_4}{\eta_3}\right)s_1c_2s_3s_4c_5$$
$$- \left(\frac{\eta_{in}\eta_s\eta_3}{\eta_1\eta_5}+\frac{\eta_1\eta_5}{\eta_3}\right)s_1c_2s_3c_4s_5 - \left(\frac{\eta_{in}\eta_s\eta_4}{\eta_1\eta_5}+\frac{\eta_1\eta_5}{\eta_4}\right)s_1c_2c_3s_4s_5$$
$$- \left(\frac{\eta_{in}\eta_s\eta_3}{\eta_2\eta_4}+\frac{\eta_2\eta_4}{\eta_3}\right)c_1s_2s_3s_4c_5 - \left(\frac{\eta_{in}\eta_s\eta_3}{\eta_2\eta_5}+\frac{\eta_2\eta_5}{\eta_3}\right)c_1s_2s_3c_4s_5$$
$$- \left(\frac{\eta_{in}\eta_s\eta_4}{\eta_2\eta_5}+\frac{\eta_2\eta_5}{\eta_4}\right)c_1s_2c_3s_4s_5 - \left(\frac{\eta_{in}\eta_s\eta_4}{\eta_3\eta_5}+\frac{\eta_3\eta_5}{\eta_4}\right)c_1c_2s_3s_4s_5$$
$$\left.+ \left(\frac{\eta_{in}\eta_s\eta_2\eta_4}{\eta_1\eta_3\eta_5}+\frac{\eta_1\eta_3\eta_5}{\eta_2\eta_4}\right)s_1s_2s_3s_4s_5\right], \qquad \text{(A.19)}$$

Now, both numerator and denominator contain $1 + C_{5,2} + C_{5,4} = 16$ terms (for the RP) and $C_{5,1} + C_{5,3} + C_{5,5} = 16$ terms for the IP (i.e., the total number of summands is $S_5 = 2^4$).

Assuming that $S_k = 2^{k-1}$, it is trivially found (by mathematical induction) that the total number of terms for $k + 1$ layers results to be $S_{k+1} = 2^k$.

References

[1] Chen K M, Sparks A W, Luan H-C, Lim D R, Wada K and Kimerling L C 1999 *Appl. Phys. Lett.* **75** 3805
[2] Lee H Y, Makino H, Yao T and Tanaka A 2002 *Appl. Phys. Lett.* **81** 4502
[3] Deopura M, Ullal C K, Temelkuran B and Fink Y 2001 *Opt. Lett.* **26** 1197

[4] Zhukovsky S V 2010 it Phys. Rev. A **81** 053808
[5] Kalozoumis P A, Morfonios C, Palaiodimopoulos N, Diakonos F K and Schmelcher P 2013 *Phys. Rev. A* **88** 033857
[6] Kärtner F X, Morgner U, Ell R, Schibli T, Fujimoto J G, Ippen E P, Scheuer V, Angelow G and Tschudi T 2001 *J. Opt. Soc. Am. B* **18** 882-885
[7] Barriuso A G, Monzon J J, Yonte T, Felipe A and Sanchez-Soto L L 2013 *Opt. Express* **21** 30039
[8] del Barco O, Conejero Jarque E, Gasparian V and Bueno J M 2017 *J. Opt.* **19** 065102
[9] Moretti L and Scotognella F 2015 *Opt. Mater.* **46** 450-453
[10] Abèles F 1958 *J. Phys. Radium* **19** 327-334
[11] Szipöcs R, Ferencz K, Spielmann C and Krausz F 1994 *Opt. Lett.* **19** 201-2013
[12] Nisoli M, De Silvestri S, Svelto O, Szipöcs R, Ferencz K, Spielmann C, Sartania S and Krausz F 1997 *Opt. Lett.* **22**, 522-524
[13] Steinmeyer G 2006 *Appl. Opt.* **45** 1484-1490
[14] Pervak V, Razskazovskaya O, Angelov I B, Vodopyanov K L and Trubetskov M 2014 *Adv. Opt. Technol.* **3** 55-63
[15] Razskazovskaya O, Krausz F and Pervak V 2017 *Optica* **4** 129-138
[16] Pervak V 2018 *Optical coatings for high-intensity femtosecond lasers*, in Optical Thin Films and Coatings From Materials to Applications, Woodhead Publishing Series in Electronic and Optical Materials, 667-696
[17] Wirth A, Hassan M T, Grguras I, Gagnon J, Moulet A, Luu T T, Pabst S, Santra R, Alahmed Z A, Azzeer A M, Yakovlev V S, Pervak V, Krausz F and Goulielmakis E 2011 *Science* **334** 195-200
[18] Huang S-W, Cirmi G, Moses J, Hong K-H, Bhardwaj S, Birge J R, Chen L-J, Li E, Eggleton B J, Cerullo G and Kärtner F X 2011 *Nat. Photonics* **5** 475-479
[19] Silva F, Alonso B, Holgado W, Romero R, San Román J, Conejero Jarque E, Koop H, Pervak V, Crespo H and Sola I J 2018 *Opt. Lett.* **43** 337-340
[20] Suman M, Monaco G, Pelizzo M G, Windt D L and Nicolosi P 2009 *Opt. Express* **17** 7922-7932
[21] Hofstetter M, Schultze M, Fiess M, Dennhardt B, Guggenmos A, Gagnon J, Yakovlev V S, Goulielmakis E, Kienberger R, Gullikson E M, Krausz F and Kleineberg U 2011 *Opt. Express* **19** 1767-1776
[22] Bourassin-Bouchet C, De Rossi S, Wang J, Meltchakov E, Giglia A, Mahne N, Nannarone S and Delmotte F 2012 *New J. Phys.* **14** 023040
[23] Chia S-H, Cirmi G, Fang S, Rossi G M, Mücke O D and Kärtner F X 2014 *Optica* **1** 315-333
[24] Habel F and Pervak V 2017 *Appl. Opt.* **56** C71-C74
[25] Pervak V, Amotchkina T, Wang Q, Pronin O, Mak K F and Trubetskov M 2019 *Opt. Express* **27** 55-62
[26] Chen L-J, Chang G, Li C-H, Benedick A J, Philips D F, Walsworth R L and Kärtner F X 2010 *Opt. Express* **18** 23204-23211
[27] Habel F, Shirvanyan V, Trubetskov M, Burger C, Sommer A, Kling M F, Schultze M and Pervak V 2016 *Opt. Express* **24** 9218-9223
[28] Wang Z, Mu H, Yuan J, Zhao C, Bao Q and Zhang H 2016 *IEEE J. Sel. Top. Quantum Electron.* **23** 195-199
[29] Jiang X, Liu S, Liang W, Luo S, He Z, Ge Y, Wang H, Cao R, Zhang F, Wen Q, Li J, Bao Q, Fan D and Zhang H 2017 *Laser Photonics Rev.* **12** 1700229
[30] Song Y, Liang Z, Jiang X, Chen Y, Li Z, Lu L, Ge Y, Wang K, Zheng J, Lu S, Ji J and Zhang H 2017 *2D Mater.* **4** 045010
[31] Saleh B E A and Teich M C 2007 *Fundamentals of Photonics, (Wiley Series in Pure and Applied Optics*
[32] Amotchkina T, Trubetskov M and Pervak V 2017 *Opt. Express* **25** 12675-12688
[33] Razskazovskaya O, Luu T T, Trubetskov M, Goulielmakis E and Pervak V 2015 *Optica* **2** 803-811
[34] Palmier S, Neauport J, Baclet N, Lavastre E and Dupuy G 2009 *Opt. Express* **17** 20430-20439
[35] Qiao J, Schmid A W, Waxer L J, Nguyen T, Bunkenburg J, Kingsley C, Kozlov A and Weiner D 2010 *Opt. Express* **18** 10423-10431
[36] Kong F, Jin Y, Huang H, Zhang H, Liu S and He H 2015 *Opt. Laser Technol.* **73** 39-43
[37] Negres R A, Carr C W, Laurence T A, Stanion K, Guss G, Cross D A, Wegner P J and Stolz C J 2017 *Opt. Eng.* **56** 011008

[38] MacLeod H A 2010 *Thin-film optical filters, Taylor and Francis Group*